Electronic Supplementary Information

Synthesis of indacenodithienothiophene-based conjugated polymers containing electron-donating/accepting comonomers and their phototransistor characteristics

Yejin Moon[a], Chulyeon Lee[a], Hwajeong Kim[a,b], Jisu Park[a] and Youngkyoo Kim[a,*]

[a]Organic Nanoelectronics Laboratory and KNU Institute for Nanophotonics Applications (KINPA), Department of Chemical Engineering, School of Applied Chemical Engineering, Kyungpook National University, Daegu 41566, Republic of Korea

[b]Priority Research Center, Research Institute of Environmental Science & Technology, Kyungpook National University, Daegu 41566, Republic of Korea

*Corresponding Author: Prof. Y. Kim

E-mail) ykimm@knu.ac.kr

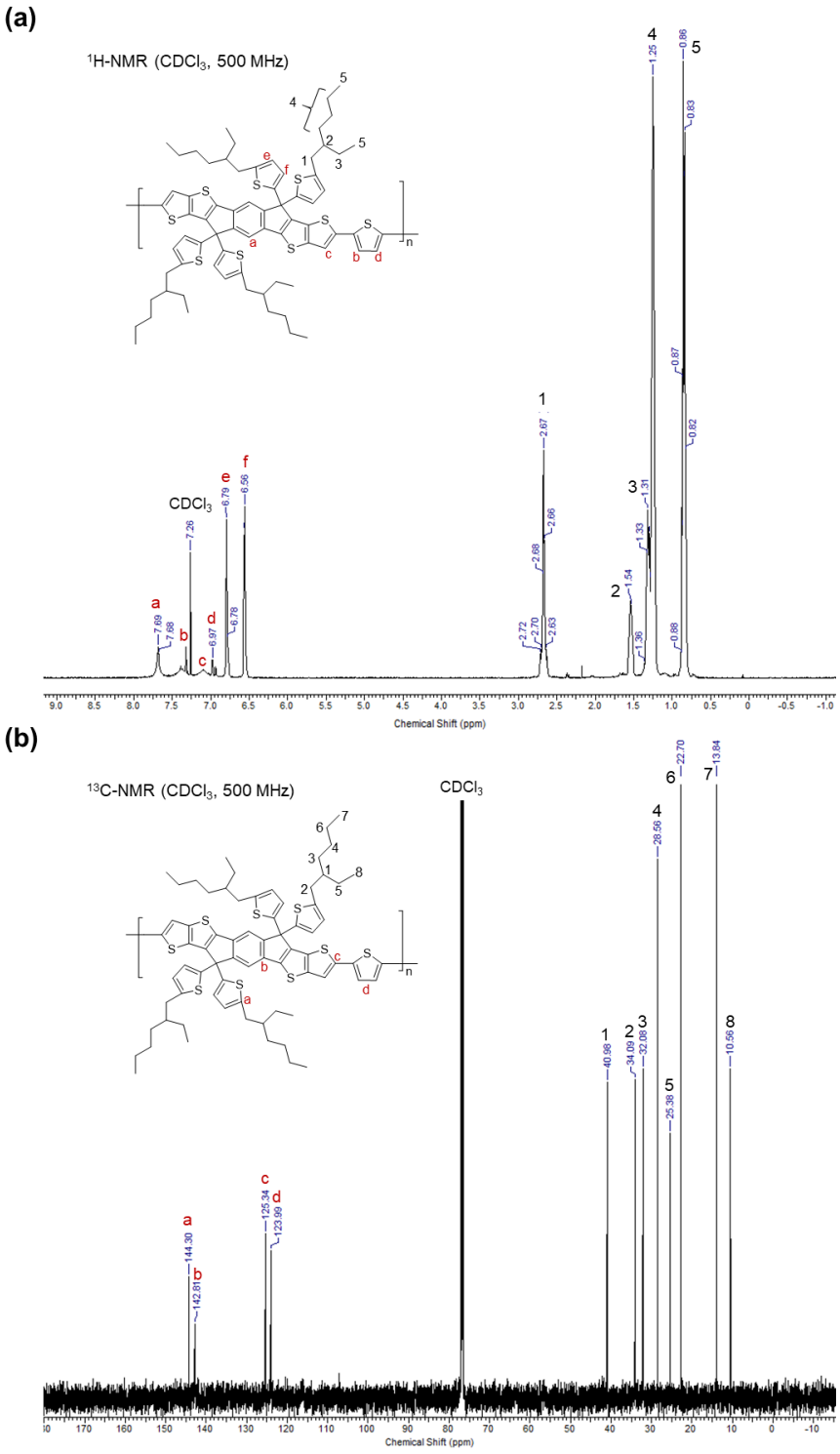

Figure S1. (a) ^{1}H-NMR and (b) ^{13}C-NMR (500 MHz) spectra for the PIDTT-Th polymer (solvent: $CDCl_3$) synthesized in this work (see the assigned peaks on the major proton atoms marked on the molecular structure).

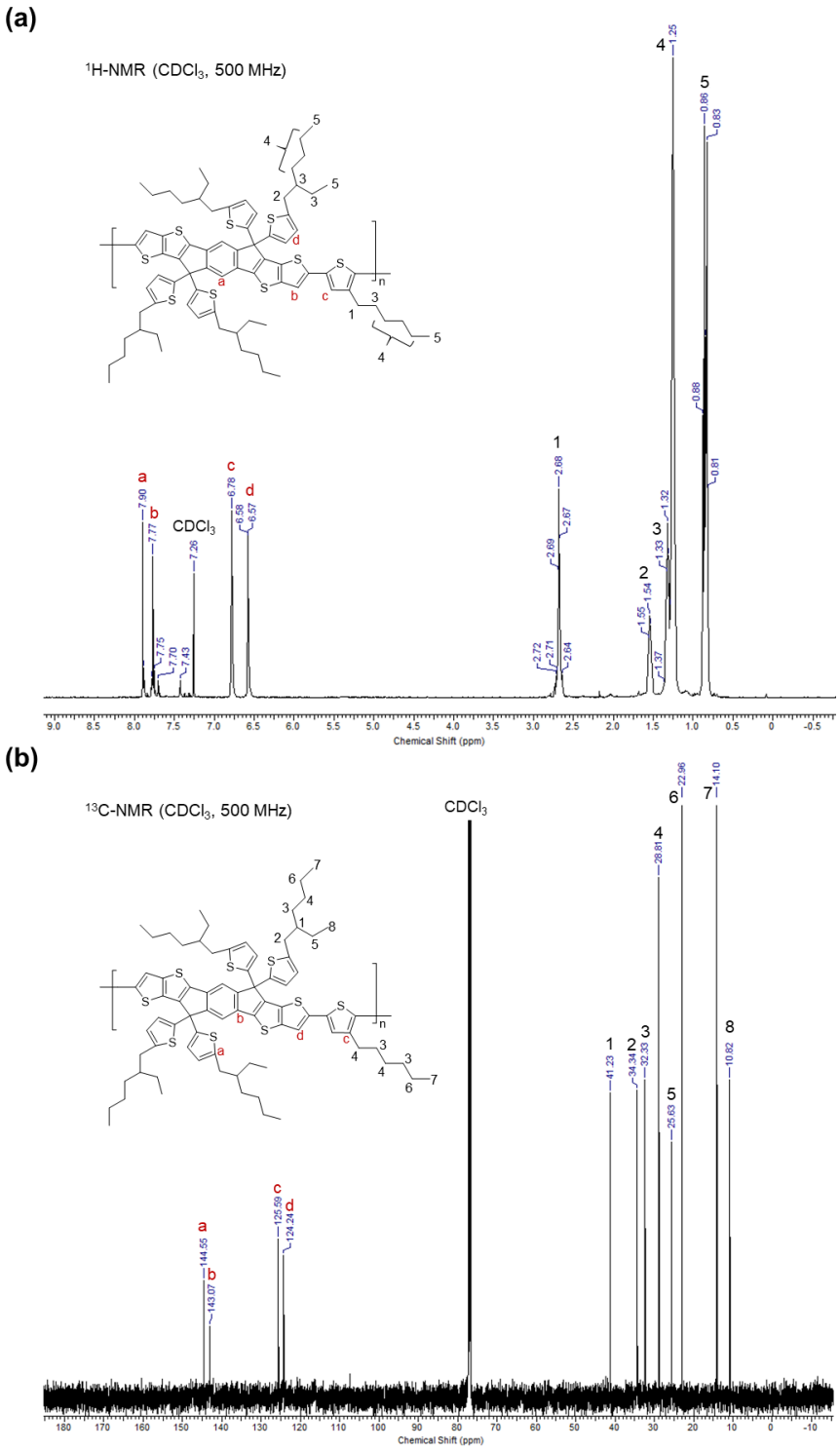

Figure S2. (a) ^{1}H-NMR and (b) ^{13}C-NMR (500 MHz) spectra for the PIDTT-3HT polymer (solvent: $CDCl_3$) synthesized in this work (see the assigned peaks on the major proton atoms marked on the molecular structure).

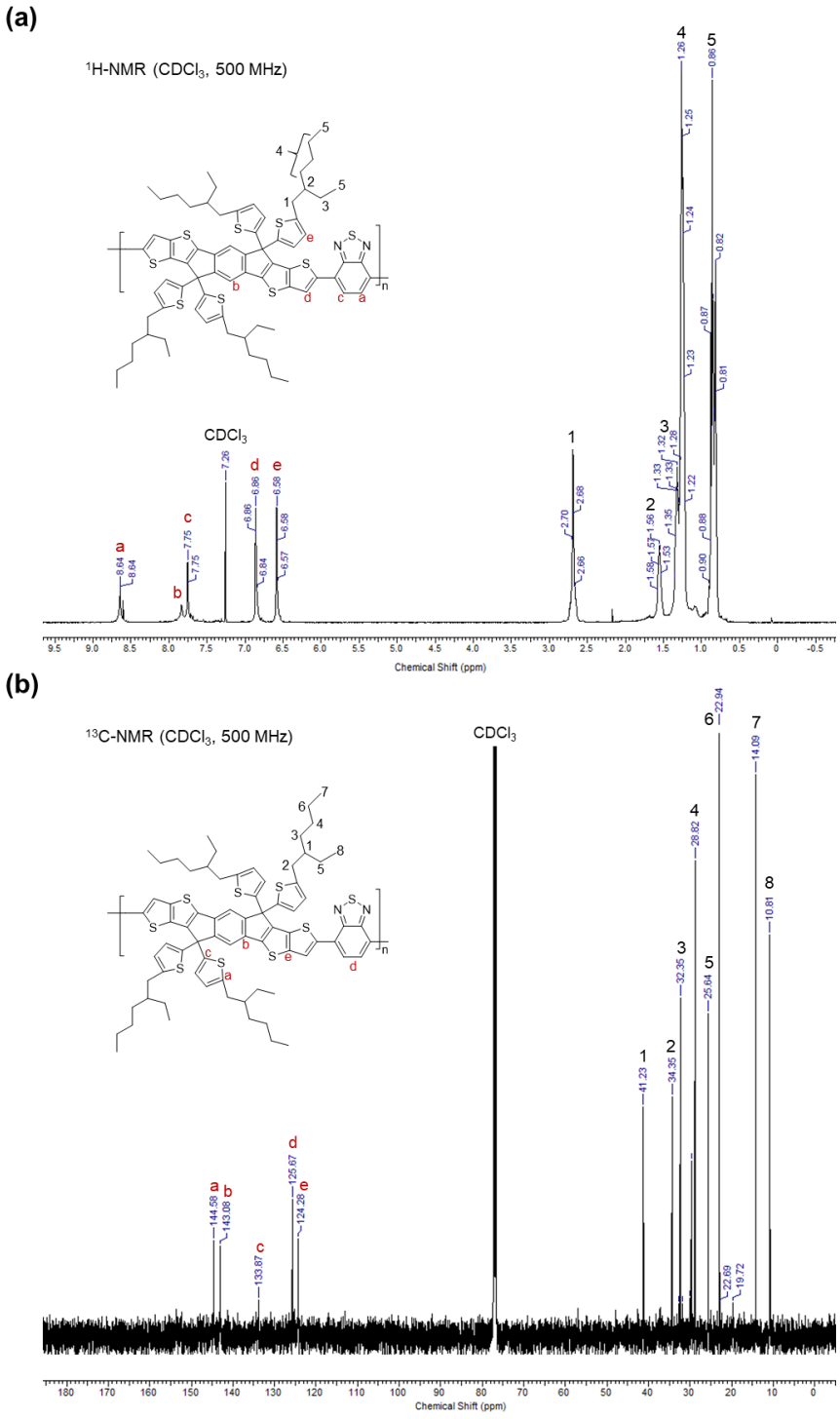

Figure S3. (a) ^{1}H-NMR and (b) ^{13}C-NMR (500 MHz) spectra for the PIDTT-BT polymer (solvent: $CDCl_3$) synthesized in this work (see the assigned peaks on the major proton atoms marked on the molecular structure).

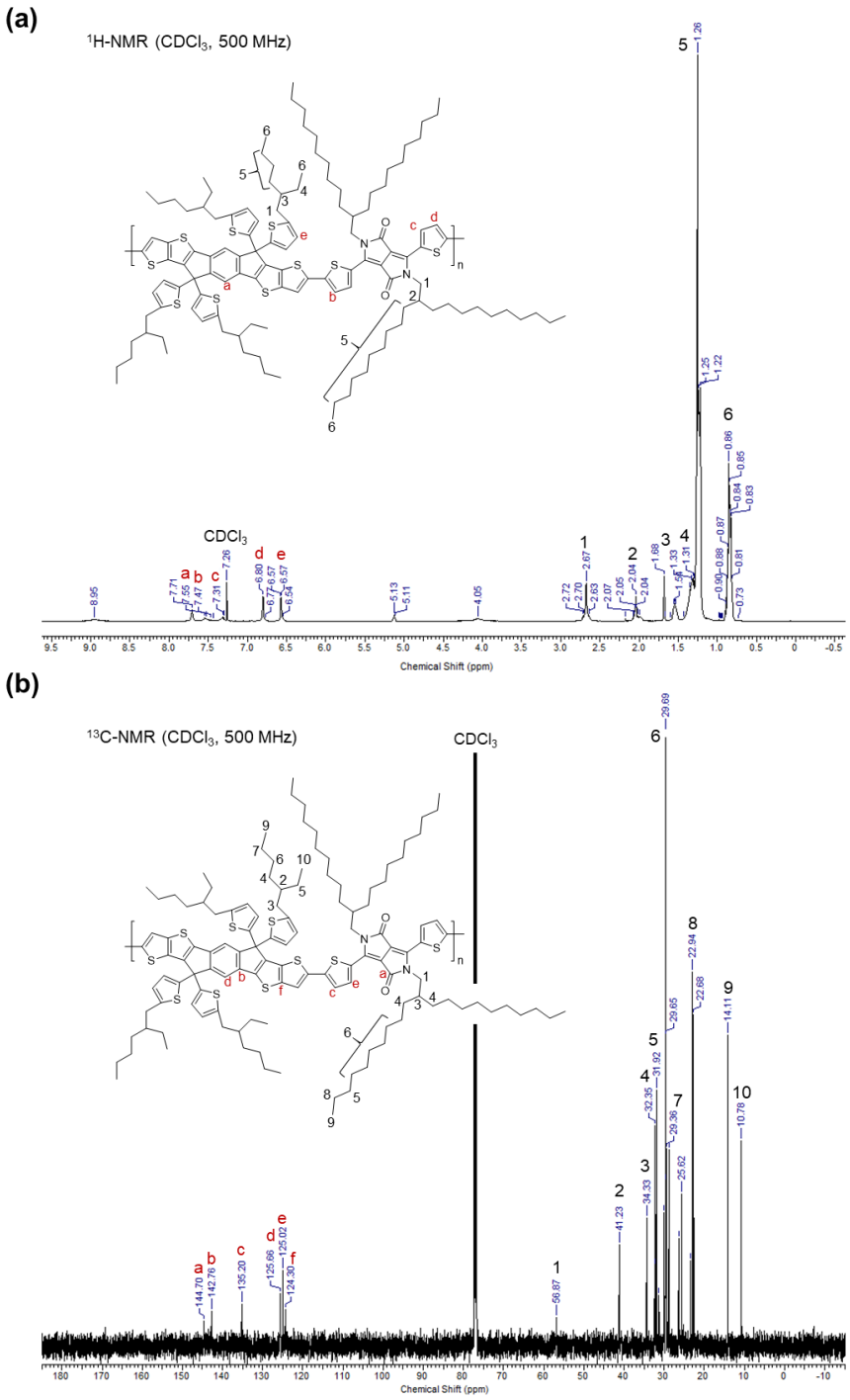

Figure S4. (a) ^{1}H-NMR and (b) ^{13}C-NMR (500 MHz) spectra for the PIDTT-DPP polymer (solvent: $CDCl_3$) synthesized in this work (see the assigned peaks on the major proton atoms marked on the molecular structure).

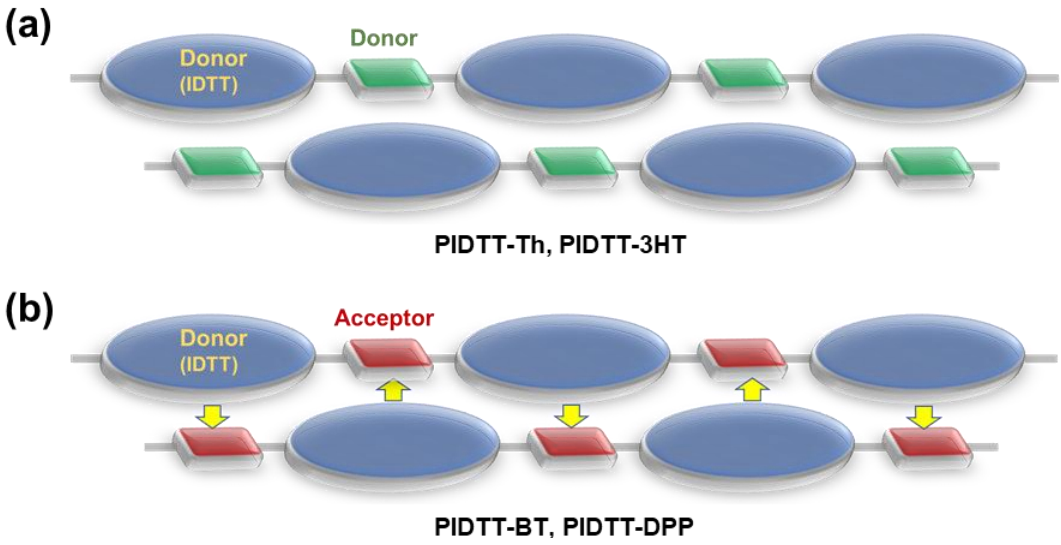

Figure S5. Illustration for the possible interchain donor-acceptor interactions of the IDTT-based polymers: (a) Polymers with all electron-donating comonomers (PIDTT-Th and PIDTT-3HT), (b) polymers with both electron-donating and electron-accepting comonomers (PIDTT-BT and PIDTT-DPP). Note that the size of IDTT and comonomer units was simply reflected for better understanding. The yellow arrows in (b) represent the donor-acceptor interactions.

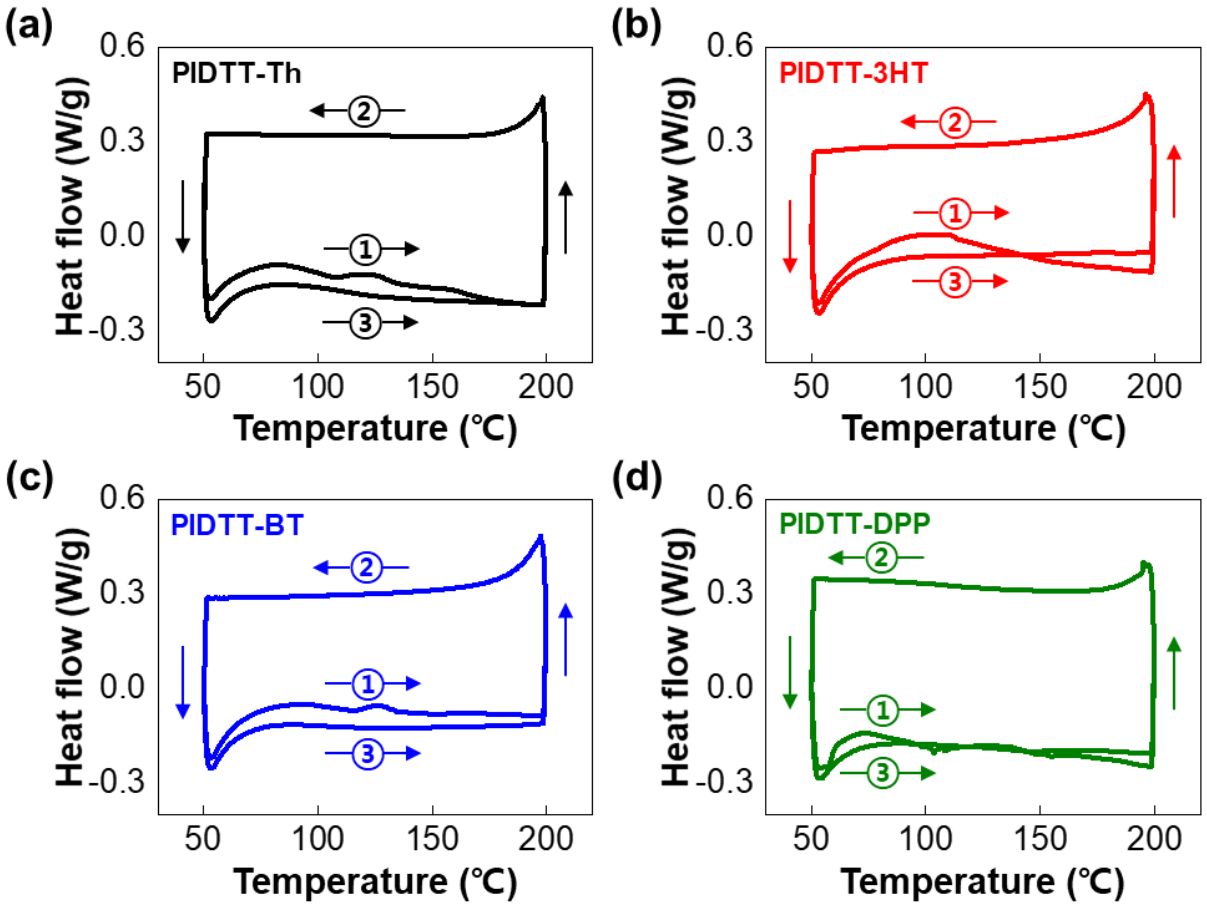

Figure S6. DSC thermograms for the IDTT-based polymers: (a) PIDTT-Th, (b) PIDTT-3HT, (c) PIDTT-BT, and (d) PIDTT-DPP. ① First run (heating): from 50 °C to 200 °C at a heating rate of 10 °C/min; ② Second run (quenching): from 200 °C to 50 °C at a heating rate of 10 °C/min; ③ Third run (heating): from 50 °C to 200 °C at a heating rate of 10 °C/min. The third run data were used for the analysis of glass transition temperature in Figure 1b after baseline correction.

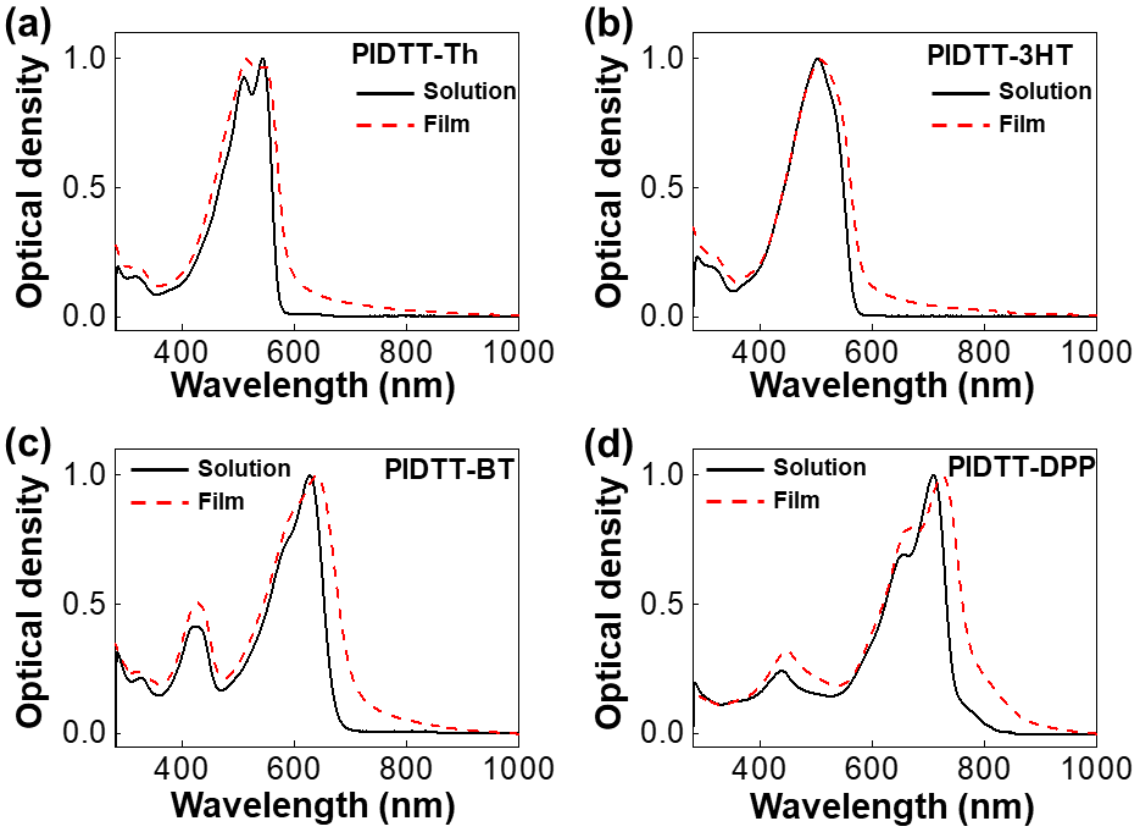

Figure S7. Optical absorption spectra for the IDTT-based polymers: (a) PIDTT-Th, (b) PIDTT-3HT, (c) PIDTT-BT, and (d) PIDTT-DPP. The concentration of solutions was 10 mg/ml in chlorobenzene, while the thickness of films was 50 nm.

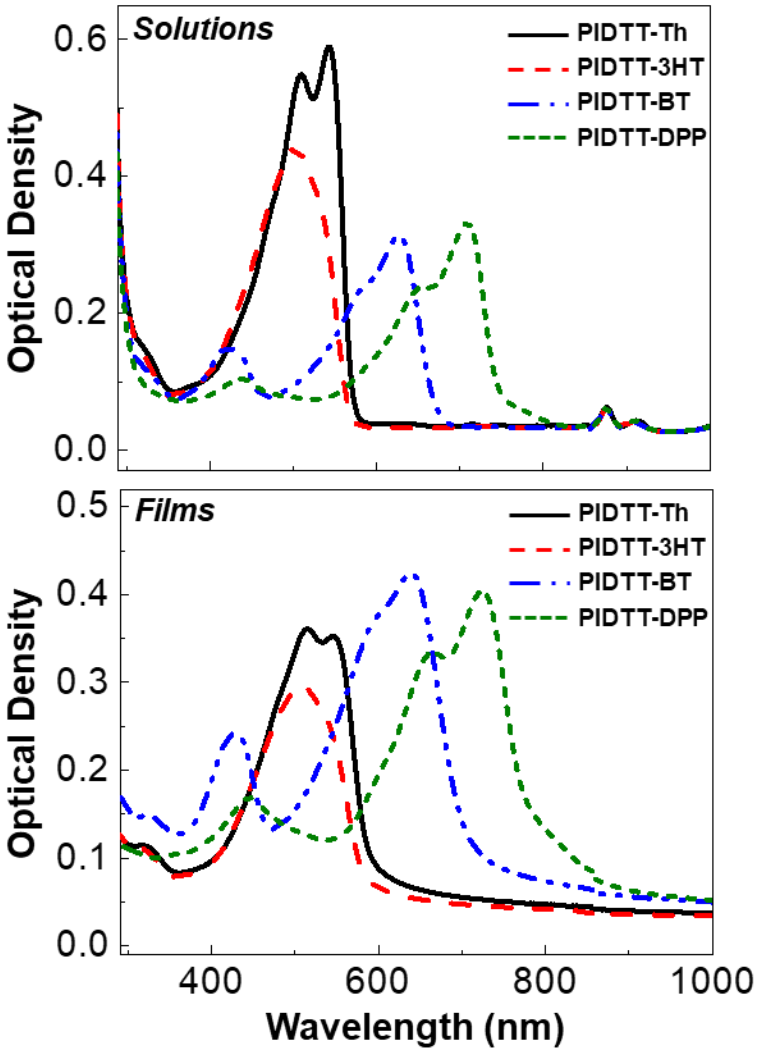

Figure S8. Optical absorption spectra (unnormalized) for the IDTT-based polymers: (top) solutions in chlorobenzene (concentration = 10 mg/ml, path length = 10 mm); (bottom) films (thickness = 50 nm).

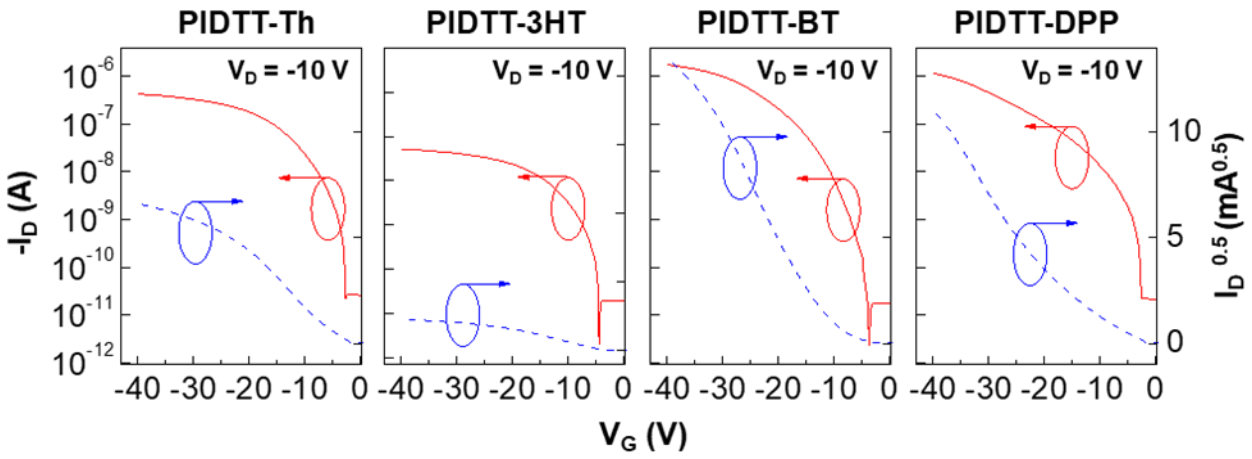

Figure S9. Transfer characteristics (V_D = -10 V) for the OFETs with the IDTT-based polymer channel layers.

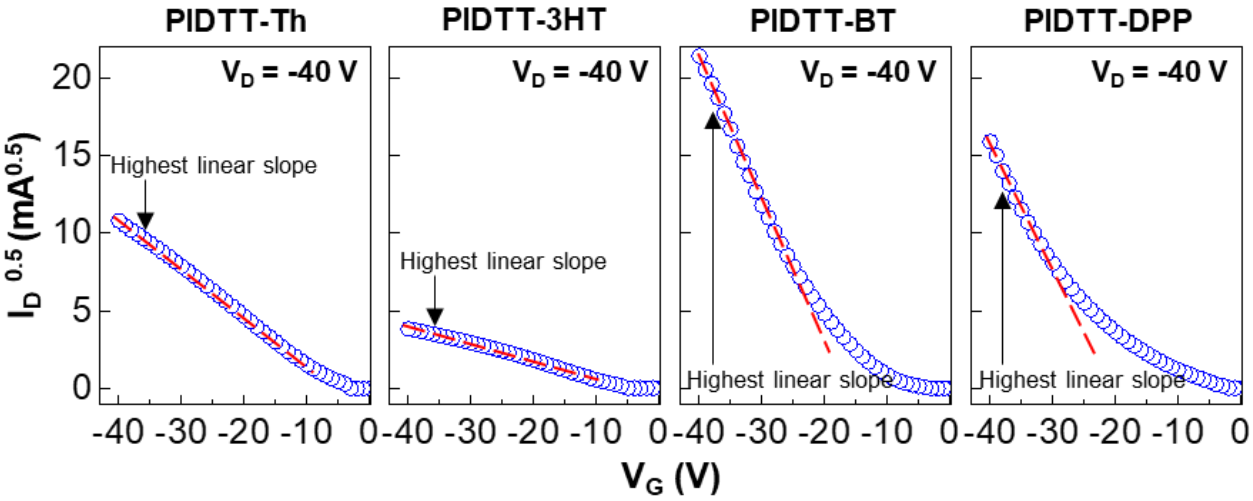

Figure S10. $I_D^{0.5}$-V_G curves for the OFETs with the IDTT-based polymer channel layers (from the transfer curves in Figure 4b). The hole mobility values in Table 2 were obtained from the highest linear slopes, which correspond to the saturation region in the output curves, by employing the saturation regime equation $\boldsymbol{I_{D,sat} = \frac{W}{2L} C_{GIL} \mu_{sat} (V_G - V_{TH})^2}$ ($\boldsymbol{I_{D,sat}}$: drain current in the saturation region; $\boldsymbol{W}$: channel width; $\boldsymbol{L}$: channel length; $\boldsymbol{C_{GIL}}$: capacitance of gate-insulating layer; $\boldsymbol{\mu_{sat}}$: hole mobility in the saturation region).

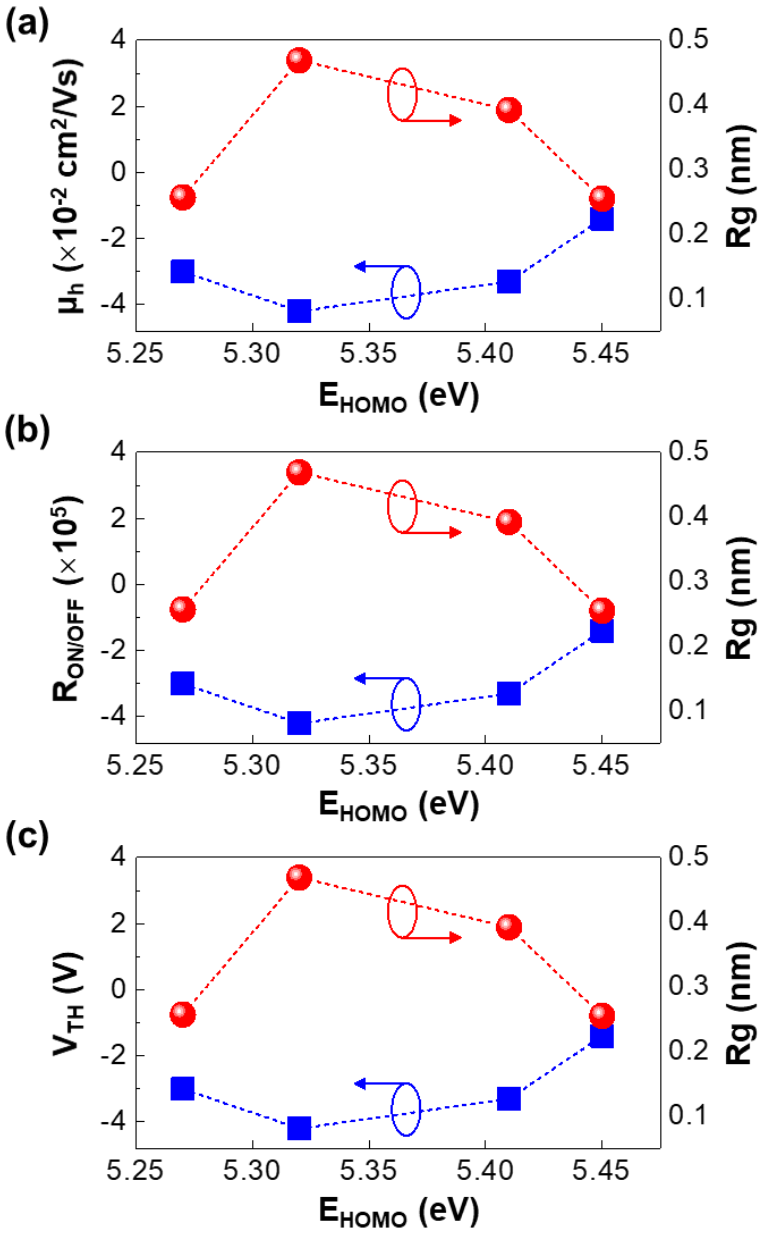

Figure S11. Correlation between transistor parameters and roughness (Rg) as a function of the HOMO energy levels that are taken from Table 1 for each IDTT-based polymer: (a) hole mobility (μ_h) versus Rg, (b) on/off ratio ($R_{ON/OFF}$) versus Rg, (c) threshold voltage (V_{TH}) versus Rg. Note that the transistor parameters were obtained from the transfer curves at V_G = -40 V and V_D = -40 V.

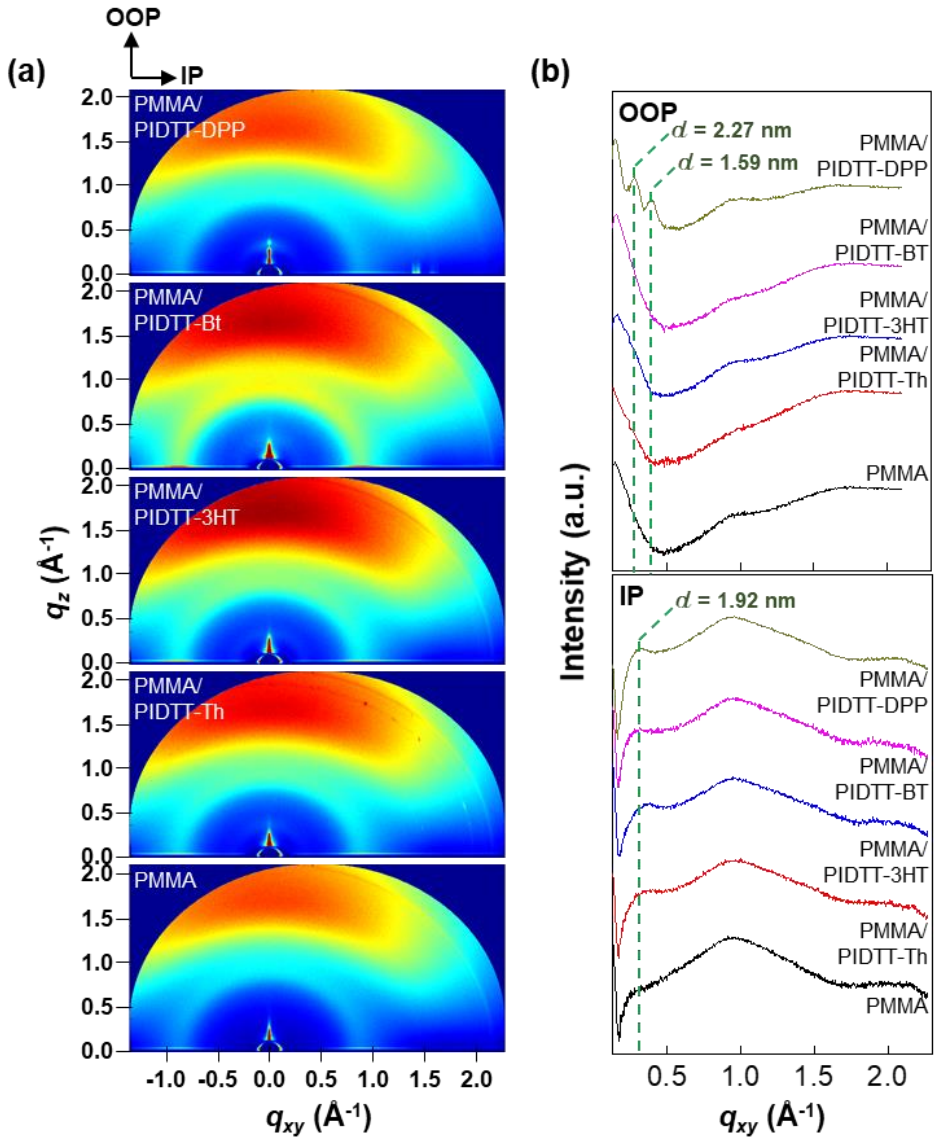

Figure S12. GIWAXS results for the IDTT-based polymer films (thickness = 50 nm) coated on the PMMA layers: (a) 2D GIWAXS images, (b) 1D GIWAXS profiles (top: OOP direction; bottom: IP direction). The d-spacing (*d*) values are given on each graph in (b).

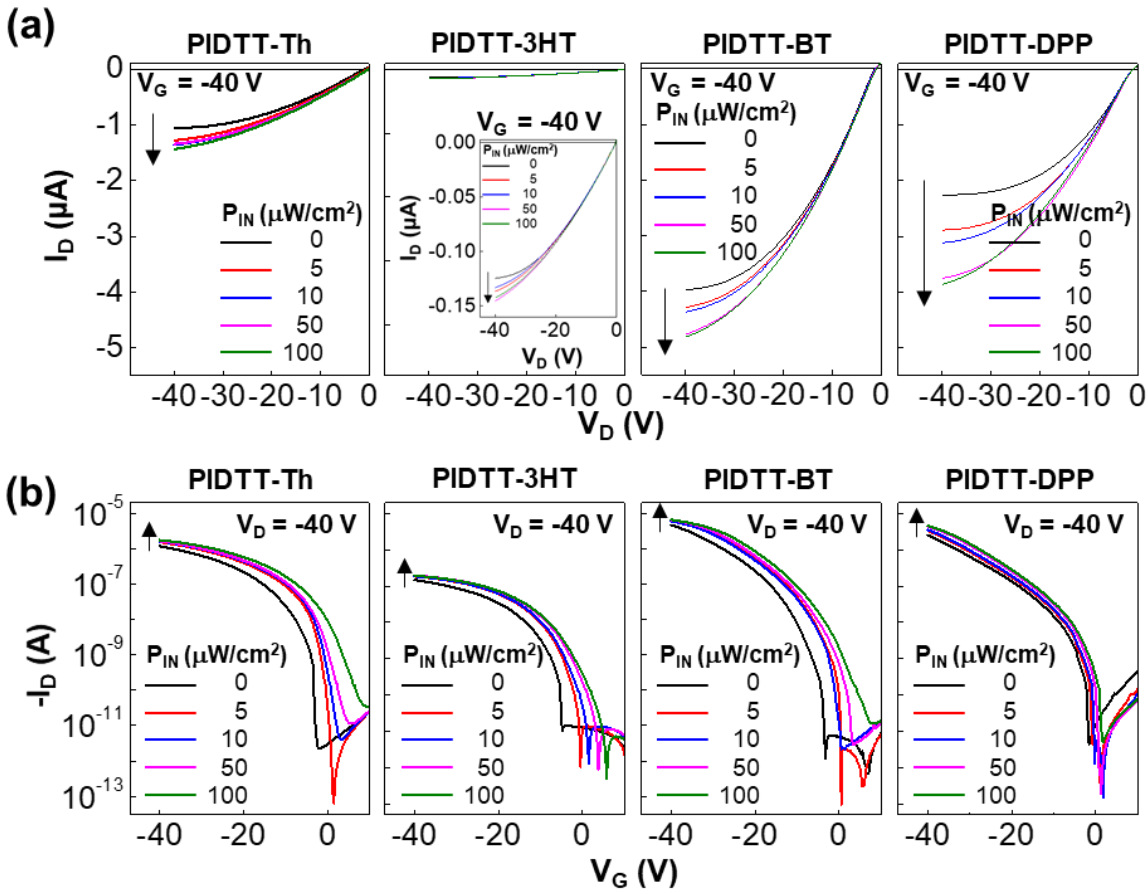

Figure S13. Photosensing characteristics (full data) for the OFETs with the IDTT-based polymer channel layers: (a) output curves, (b) transfer curves. The wavelength of incident light was 510, 510, 640, 720 nm for PIDTT-Th, PIDTT-3HT, PIDTT-BT, and PIDTT-DPP, respectively. The incident light intensity (P_{IN}) was varied at the fixed wavelength for each case (see the arrow for the direction of P_{IN} increase).

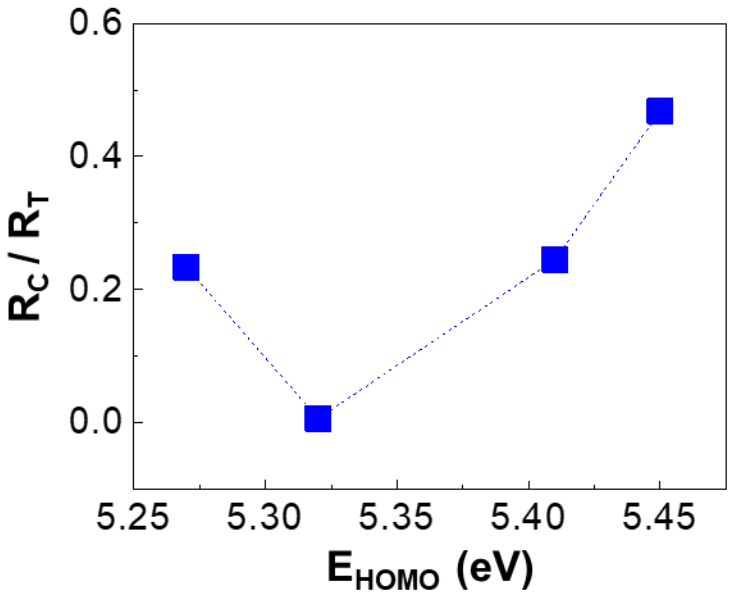

Figure S14. Theoretical limit (R_T)-normalized photoresponsivity (R_C/R_T) according to the HOMO energy level (eV). The theoretical limit of photoresponsivity (R_T) is 5.27, 5.32, 5.41and 5.45 eV at 510, 510, 640, 720 nm, respectively. Refs: (1) J. Wu, G. K. W. Koon, D. Xiang, C. Han, C. T. Toh, E. S. Kulkarni, I. Verzhbitskiy, A. Carvalho, A. S. Roding, S. P. Koenig, G. Eda, W. Chen, A. H. C. Neto and B. Ozyilmaz, *ACS Nano* 2015, **9**, 8070; (2) H. Han, S. Nam, J. Seo, C. Lee, H. Kim, D. D. C. Bradley, C.-S. Ha and Y. Kim, *Sci. Rep.* 2015, **5**, 16457.

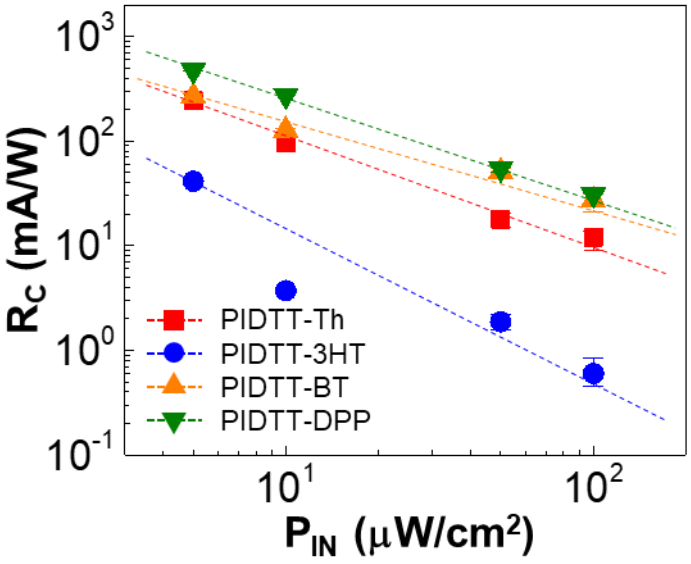

Figure S15. Corrected photoresponsivity (R_C) as a function of incident light intensity (P_{IN}) for the OFETs with the IDTT-based polymer channel layers. Note that the R_C values were obtained from the transfer curves at V_G = -40 V and V_D = -40 V.